

# Soluble MHC-Peptide Complexes Induce Rapid Death of CD8<sup>+</sup> CTL<sup>1</sup>

Marek Cebecauer,\* Philippe Guillaume,\* Pavel Hozák,<sup>†</sup> Silke Mark,\* Helen Everett,<sup>‡</sup> Pascal Schneider,<sup>‡</sup> and Immanuel F. Luescher<sup>2\*</sup>

Soluble MHC-peptide (pMHC) complexes, commonly referred to as tetramers, are widely used to enumerate and to isolate Ag-specific CD8<sup>+</sup> CTL. It has been noted that such complexes, as well as microsphere- or cell-associated pMHC molecules compromise the functional integrity of CTL, e.g., by inducing apoptosis of CTL, which limits their usefulness for T cell sorting or cloning. By testing well-defined soluble pMHC complexes containing linkers of different length and valence, we find that complexes comprising short linkers (i.e., short pMHC-pMHC distances), but not those containing long linkers, induce rapid death of CTL. This cell death relies on CTL activation, the coreceptor CD8 and cytoskeleton integrity, but is not dependent on death receptors (i.e., Fas, TNFR1, and TRAILR2) or caspases. Within minutes of CTL exposure to pMHC complexes, reactive oxygen species emerged and mitochondrial membrane depolarized, which is reminiscent of caspase-independent T cell death. The morphological changes induced during this rapid CTL death are characteristic of programmed necrosis and not apoptosis. Thus, soluble pMHC complexes containing long linkers are recommended to prevent T cell death, whereas those containing short linkers can be used to eliminate Ag-specific CTL. *The Journal of Immunology*, 2005, 174: 6809–6819.

The engagement of TCR and the coreceptor CD8 (or CD4) by peptide-MHC class I (pMHC)<sup>3</sup> complexes expressed on other cells largely determines the development, differentiation, and homeostasis of T cells (1). In the periphery, this interaction primarily controls the activation and differentiation of T lymphocytes. The studies of T cell activation also demonstrated that TCR-pMHC interaction can lead to apoptosis of T cells to maintain homeostasis (2). One form of such T cell deletion is activation-induced cell death by Fas (CD95)-dependent mechanisms (3). For mature CD8<sup>+</sup> T cells, TCR-induced apoptosis can also be mediated by the TNFR (4). More recently activated T cell-autonomous death (ACAD) has been described, which is Fas ligand- and TNF- $\alpha$ -independent and primarily eliminates activated T cells that express low levels of Bcl2 (5). An emerging consensus is that activation-induced cell death mediates apoptosis of T cells exposed to persistent Ags, such as autoantigens or pathogens causing chronic infections. Conversely, ACAD is thought to be mainly responsible for the elimination of activated T cells during the con-

traction phase of strong immune response to transient stimuli, such as viral infections (6). ACAD involves activation-induced generation of reactive oxygen species (ROS) and depolarization of mitochondrial membranes (7). Decreased expression of antiapoptotic molecules (e.g., Bcl-2) renders T cells susceptible for this mitochondrial dysfunction-dependent death (6).

Fluorescent-labeled soluble pMHC class I complexes, termed tetramers or dimeric fusion proteins of pMHC with an Ig, are widely used to enumerate and isolate Ag-specific CD8<sup>+</sup> T cells (8, 9). It has been noted that such reagents affect the functional integrity of T cells (10–12), which is a concern when considering fluorescence-activated cell sorting or cloning of such cells. This is especially true for activated effector CTL that are susceptible to activation-dependent cell death as seen, for example, in the contraction phase after viral infection, when large numbers of antiviral CTL are eliminated to re-establish homeostasis (2). Although it is known that soluble pMHC complexes can kill Ag-specific CTL, it is not clear by what mechanism(s). So far, two mechanisms have been described. First, cognate pMHC complexes expressed on target cells or microspheres (12) or as soluble pMHC complexes (10, 12) have been shown to induce Fas-dependent apoptosis of effector CTL. Induction of CTL apoptosis does not require coengagement of CD8 by pMHC, nor significant Lck activation, intracellular calcium mobilization, or tyrosine phosphorylation (10, 12). It has therefore been suggested that CD8 binding-deficient pMHC complexes can be used to eliminate Ag-specific CTL in the absence of systemic, potentially harmful CTL activation. Second, peptide can be transferred from soluble to CTL-associated MHC molecules and thus sensitize CTL for fratricide killing (13–15). Although the mechanism of this peptide transfer remains to be elucidated, it is a serious concern, especially when CTL are incubated for longer periods of time with soluble pMHC complexes.

Soluble pMHC complexes, both of class I and class II, also have been used as immunomodulatory agents. For example, dimeric pMHC class II complexes have been shown to blunt autoreactive T cell responses in animal models of diabetes type I and encephalomyelitis (16–18). Dimeric pMHC class I complexes have been

\*Ludwig Institute for Cancer Research, Lausanne Branch, Epalinges, Switzerland; <sup>†</sup>Institute of Experimental Medicine, Academy of Sciences of the Czech Republic, Prague, Czech Republic; and <sup>‡</sup>Department of Biochemistry, University of Lausanne, Epalinges, Switzerland

Received for publication December 23, 2004. Accepted for publication March 24, 2005.

The costs of publication of this article were defrayed in part by the payment of page charges. This article must therefore be hereby marked *advertisement* in accordance with 18 U.S.C. Section 1734 solely to indicate this fact.

<sup>1</sup>This study was supported by grants from Swiss National Foundation (no. 31-1946.00) and the Stanley Thomas Foundation.

<sup>2</sup>Address correspondence and reprint requests to Dr. Immanuel F. Luescher, Ludwig Institute for Cancer Research, Lausanne Branch, 1066 Epalinges, Switzerland. E-mail address: immanuel.luescher@isrec.unil.ch

<sup>3</sup>Abbreviations used in this paper: pMHC, peptide-MHC class I; ACAD, activated T cell-autonomous death; ROS, reactive oxygen species; PbCS, *Plasmodium berghei* circumsporozoite; ABA, 4-azidobenzoic acid; TMRM, tetramethylrhodamine methyl ester; HE, dihydroethidium; DHR, dihydrorhodamine 123; DiOC<sub>6</sub>, 3,3'-dihexyloxycarbocyanine iodide; 7AAD, 7-aminoactinomycin D; Dabco, 1,4-diazabicyclo [2.2.2]octane; COX, cytochrome oxidase; Dap, diaminopropionic acid; PS, phosphatidylserine;  $\Delta\psi_m$ , mitochondrial membrane potential; PKC, protein kinase C; BNIP3, Bcl-2/adenovirus E1B 19-kDa protein-interacting protein 3.

reported to inhibit CTL-mediated cytotoxicity *in vivo* (19, 20). The underlying mechanism of this inhibition is not known, and because it exhibited degenerate specificity, it may involve pMHC-induced death of the CTL.

The present study was undertaken to investigate how soluble pMHC complexes affect CTL viability. Such reagents are prepared by reacting biotinylated pMHC monomers with PE- or allophycocyanin-labeled streptavidin (8). Due to heterogeneities in these streptavidin preparations, such reagents are ill-defined mixtures of different pMHC complexes (10), hereafter referred to as multimers. To prepare well-defined dimeric, tetrameric, and octameric pMHC complexes, we used site-specific alkylation with linkers containing spacers of different length, i.e., different pMHC-pMHC distances (10, 21). For long spacers, we used polyprolines, which in aqueous solution assume rigid proline II helices, in which one residue spans 3.1 Å (22). As cells, we used cloned S14 CTL and CD8<sup>+</sup> T cells from T1 TCR transgenic mice, which recognize the *Plasmodium berghei* circumsporozoite (PbCS) peptide 252–260 (SYIPSAEKI) containing photoreactive 4-azidobenzoic acid (ABA) on K259 (PbCS(ABA)) in the context of K<sup>d</sup> (23, 24). The PbCS(ABA) variants containing alanine or leucine in place of proline 255 are strong agonists for S14 and T1 CTL, respectively (25). We report that pMHC complexes containing short, but not those containing long linkers, induce rapid nonapoptotic death of CTL. The new findings are discussed in the context of previously described death mechanisms for T cells, and ways are shown how appropriate pMHC complexes can be used either to eradicate Ag-specific CTL or to avoid this.

## Materials and Methods

### Reagents, cells, and mice

All standard chemicals were purchased from Sigma-Aldrich, Merck, and Alexis Biochemicals; tetramethylrhodamine methyl ester (TMRM), dihydroethidium (HE), dihydrorhodamine 123 (DHR), and 3,3'-dihydroxycarboxyanine iodide (DiOC<sub>6</sub>) were from Molecular Probes, and 7-aminoactinomycin D (7AAD) and 1,4-diazabicyclo[2.2.2]octane (Dabco) were from Sigma-Aldrich. MitoQ was a kind gift of Dr. M. Murphy (Medical Research Council, Cambridge, U.K.). Cloned S14 CTL were cultured and used as described (23–25). T1 TCR Tg mice (RAG-2<sup>-/-</sup>) were from Dr. E. Palmer (University of Basel, Basel, Switzerland) (24) and handled according to Swiss federal guidelines. Effector T1 T cells were obtained by injecting T1 TCR Tg mice *i.v.* with 50 nmol of PbCS(ABA) peptide 2 days before harvesting their splenocytes, which were cultured in IL-2 (30 U/ml)-containing medium for another 4–7 days. "Naive T cells" refers to splenocytes from nonprimed T1 TCR Tg mice. Anti-actin rabbit polyclonal Ab was from Sigma-Aldrich, anti-cytochrome oxidase (COX) subunit IV mAb (20E8) was from Molecular Probes, and anti-cytochrome *c* (7H8.2C12) was from Apotech. The soluble death receptor-Fc fusion proteins (Fas-Fc, TRAILR2-Fc, and TNFR1-Fc) were produced and used as described (26, 27).

### Preparation of soluble K<sup>d</sup>-peptide molecules

Monomeric K<sup>d</sup>-PbCS(ABA) complexes, and its mutant K<sup>d</sup>D227K-PbCS(ABA) (charge inversion in position 227), containing either a C-terminally added BirA substrate peptide or a free cysteine in position 275 were prepared by refolding of H chain and human β<sub>2</sub>-microglobulin in the presence of peptide as described (10). As peptides, either the wild-type PbCS(ABA) (SYIPSAEK(ABA)I), PbCS(ABA)P255A (SYIASAEK(ABA)I), which is a strong agonist for S14 CTL, PbCS(ABA)P255L (SYILSAEK(ABA)I), which is a strong agonist for T1 CTL (25), or the irrelevant Cw3 170–179 peptide (RYLKNGKETL) were used. The linkers used for the preparation of the pMHC complexes were as follows: for diaminopropionic acid (Dap)S dimer, maleimidoacetoxy-S-Dap(S-maleimidoacetoxy)-Y-D-K(Cy5)-P (I); for P<sub>30</sub> dimer, Cy5-Dap(maleimidoacetoxy)-P<sub>30</sub>-Dap(maleimidoacetoxy)-P (II); for PEO tetramer, biotinyl-iodoacetamidyl-3,6-dioxaoctanediamine (Pierce Biotechnology); for P<sub>24</sub> tetramer, biotin-Y-P<sub>24</sub>-Dap(maleimidoacetoxy biotin)-P (III); and for DapS/P10 octamer, maleimidoacetoxy-S-Dap(S-maleimidoacetoxy)-Y-P<sub>10</sub>-K(biotin)-P (IV). All linkers were synthesized on solid phase using proline-2-chlorotrityl resin (Novabiochem), Fmoc for transient protection, and very acid labile orthogonal protection groups. Biotin was introduced by using Fmoc-K(biotin)

(Bachem). Sequential couplings were performed with 2.5 M excess of the respective amino acids and monitored with the chloranil color test. After each coupling, end-capping was performed with a 20-fold molar excess of acetic anhydride and di-isopropylethylamine. For I and IV, the last coupling reaction was with *N*-(α-maleimidoacetoxy)succinimide ester (Pierce) in dimethylformamide/2,4,6-collidine 1/0.01 (v/v) for 4 h at room temperature; for II, with Cy5-hydroxysuccinimide ester in dimethylformamide/DMSO/di-isopropylethylamine 1/0.1/0.01 (v/v/v) for 12 h at room temperature; and for III, likewise with biotin hydroxysuccinimide ester. Peptides were cleaved from the resin with 5% trifluoroacetic acid in dichloromethane containing 5% tri-isopropylsilane and purified on a semipreparative C4 column (Vydac), which was eluted with a linear gradient of CH<sub>3</sub>CN rising from 0 to 75% in 60 min at a flow rate of 4 ml/min. The purified peptides were characterized by mass spectrometry on a Voyager DE MALDI-TOF mass spectrometer (Applied Biosystems). For I, the purified peptide was then reacted at the free amino group with a 2-fold molar excess of Cy5 hydroxysuccinimide esters, and for II and III, with a 10-fold molar excess of *N*-(α-maleimidoacetoxy)succinimide ester. The products were purified by precipitation with ether, by gel filtration on Superdex Peptide column (Amersham Biosciences), and by chromatography on a C4 reverse-phase HPLC column, and characterized by mass spectrometry.

Dimeric, tetrameric, octameric, and multimeric K<sup>d</sup>-peptide complexes were prepared by site-specific alkylation as described (10, 21). In brief, the complexes were reduced with 15 mM glutathione and reacted with a 10-fold molar excess of the respective maleimide linkers or with Cy5-maleimide (Amersham Biosciences) for 2 h at room temperature under argon. The alkylated K<sup>d</sup>-PbCS(ABA) complexes were purified by gel filtration on a Superdex S75 column. Dimeric K<sup>d</sup>-PbCS(ABA) complexes were obtained by reacting the monomeric complexes with a 2-fold molar excess of reduced K<sup>d</sup>-PbCS(ABA)-Cys and purified by gel filtration on Superdex S200 column (10). Tetrameric and octameric pMHC complexes were obtained by reacting biotinylated mono- and dimeric pMHC complexes with a 4-fold molar excess with Cy5-labeled streptavidin (Amersham Biosciences) and purified by gel filtration on a Superdex 200 column. Multimeric complexes were obtained by reacting biotinylated K<sup>d</sup>-PbCS(ABA) monomers with PE streptavidin (Caltag) as described (10).

### Binding assay

For binding measurements, S14 CTL ( $5 \times 10^5$ ) were incubated for 5 min at 37°C with graded concentrations of Cy5-labeled pMHC complexes in 50 μl of FACS buffer (OptiMEM; Invitrogen Life Technologies) supplemented with 1% (w/v) BSA (fraction V; Sigma-Aldrich), 15 mM HEPES, 10 mM EDTA, and 0.02% (w/v) sodium azide. After UV irradiation (at 4°C for 30–40 s with 90-W mercury fluorescence light of 312 ± 40 nm), the cells were washed twice in cold FACS buffer, and cell-associated fluorescence was measured on a FACSCalibur flow cytometer (BD Biosciences).

### Calcium mobilization and cytotoxic assay

Intracellular calcium levels were measured by flow cytometry using the calcium sensitive dye Indo-1 and as described (28). For cytotoxicity analysis, <sup>51</sup>Cr-labeled P815 cells ( $5 \times 10^3$  cell/well) were incubated in microtiter plates containing 10-fold dilutions of SYIPSAEK(ABA)I peptide in DMEM supplemented with 5% FCS and 10 mM HEPES. S14 CTL ( $1.5 \times 10^4$  cells/well) were added after 5 min and after 4 h of incubation at 37°C, the released chromium was measured in supernatants. The specific lysis in percentage was calculated as follows: (experimental release – spontaneous release/total release – spontaneous release) × 100. The total release of <sup>51</sup>Cr was measured upon lysis of the target cells in 1% SDS. For inhibition assay, S14 CTL were preincubated with pMHC complexes for 30 min at 37°C before addition of the target cells. For bystander killing assay, un-sensitized target cells were used, and CTL were pretreated or not with 20 μM brefeldin A for 2 h at 37°C.

### Cell death and DNA fragmentation assays

S14 CTL or T1 T cells ( $1 \times 10^5$ ), preincubated with 20 μM brefeldin A (2 h, 37°C), were incubated with pMHC complexes for different periods of time at 37°C, washed with PBS, stained with Cy5- or FITC-labeled annexin V and 7AAD according to the manufacturer's recommendations (BD Biosciences) and analyzed by flow cytometry. Of note, Cy5-labeled annexin V detects externalized phosphatidylserine (PS) with higher sensitivity than FITC labeled. The data were analyzed by CellQuest software (BD Biosciences). Debris was excluded on the basis of forward and side scattering and dead cells by gating out 7AAD-positive counts. DNA fragmentation was analyzed using the *In situ* Cell Death Detection kit according to the manufacturer's recommendations (Roche).

### Assessment of mitochondrial membrane potential ( $\Delta\psi_m$ ) and ROS

The fluorescent probes TMRM and DiOC<sub>6</sub> were used to measure  $\Delta\psi_m$  loss. S14 CTL or effector T1 T cells ( $1 \times 10^5$ ), preincubated with 20  $\mu$ M brefeldin A for 2 h at 37°C, were incubated or not with pMHC complexes, and were then incubated with 100 nM TMRM or 40 nM DiOC<sub>6</sub> together with 2  $\mu$ g/ml 7AAD for 30 min at 37°C, and the  $\Delta\psi_m$ -dependent fluorescence was measured by flow cytometry (LSR; BD Biosciences) in the 7AAD-negative population. For ROS measurements, the same procedure was used except that ROS-sensitive probes, 10  $\mu$ M DHR or 5  $\mu$ M HE, were used. Data were processed using CellQuest software.

### Cell fractionation and cytochrome c release analysis

S14 CTL ( $1 \times 10^6$  cells), untreated or upon incubation with pMHC complexes, were washed in PBS (two times) and lysed on ice in 100  $\mu$ l of digitonin lysis buffer (75 mM NaCl, 1 mM NaH<sub>2</sub>PO<sub>4</sub>, 8 mM Na<sub>2</sub>HPO<sub>4</sub> containing 190  $\mu$ g/ml digitonin and Roche's complete protease inhibitors). Samples were centrifuged at 13,000 rpm for 10 min. Supernatant (cytosolic fraction) was kept, and the pellet was lysed in OG lysis buffer (20 mM Tris-HCl, pH 8.2, containing 100 mM NaCl, 10 mM EDTA, 1% octyl  $\beta$ -D-glucopyranoside, and Roche's protease inhibitor mixture) for 30 min on ice. The nuclei were spun out at 3000  $\times$  g for 3 min. The postnuclear supernatants (membrane fraction) and cytosolic fractions were resolved on SDS-PAGE (10% reducing) and analyzed by Western blotting using Abs specific for cytochrome c, COX subunit IV (COX IV) (mitochondria marker), and actin (loading control), respectively.

### Microscopic analyses

For all microscopic analyses, S14 CTL, pretreated with 20  $\mu$ M brefeldin A, were incubated in DMEM supplemented with 2  $\mu$ g/ml  $\beta_2$ -microglobulin in the absence or presence of 12.5 nM K<sup>d</sup>-PbCS(ABA)P255A DapS dimer for different periods of time. The samples were analyzed by DC200 light microscope (Leica), and the images were processed using Photoshop 5.0 software (Adobe). Confocal microscopy was conducted on a LSM510 confocal microscope (Zeiss). S14 CTL were incubated with 12.5 nM DapS dimer for different periods of time at 37°C. After fixation with 3% paraformaldehyde and staining with Alexa 488-labeled cholera toxin subunit B, the cells were mounted in PBS containing 50% (v/v) glycerol and 0.2 M Dabco, and analyzed by confocal microscopy. Three-dimensional reconstruction was performed using Imaris software (Bitplane). For electron microscopy, S14 CTL ( $2 \times 10^7$  cells) in OptiMEM containing 10 mM PbCS peptide and 2  $\mu$ g/ml human  $\beta_2$ -microglobulin were incubated in the absence or presence of 12.5 nM DapS dimer for 15 min at 37°C. After washing, cells were fixed in 2.5% glutaraldehyde in PBS, postfixed in 1% OsO<sub>4</sub>, dehydrated in ethanol and propyleneoxide, and embedded in Durcupan/Epon mixture. Eighty-nanometer sections were contrasted with uranyl acetate and lead citrate according to Reynolds and analyzed on a Morgagni transmission electron microscope operated at 80 kV (FEI) equipped with MegaView III digital camera (SIS).

## Results

### Soluble pMHC complexes inhibit CTL-mediated cytotoxicity by killing the CTL

Based on previous reports indicating that soluble dimeric and multimeric pMHC complexes inhibit CTL-mediated cytotoxicity (19, 20), we assessed the ability of K<sup>d</sup>-PbCS(ABA)P255A DapS dimer and multimers to inhibit the lysis of PbCS(ABA)-sensitized P815 cells by cloned S14 CTL. As shown in Fig. 1, both complexes strongly inhibited target cell killing, especially at submaximal peptide concentrations.

To ascertain whether this inhibition was caused by pMHC-mediated death of the CTL, we performed flow cytometric analysis of cloned S14 CTL before and after 30-min exposure to soluble pMHC complexes. Cell debris were gated out based on forward- and side-scatter profiles (Fig. 2). The cells were stained with annexin V, which binds to externalized PS on dying cells, and 7AAD, which labels dead cells (i.e., cells with permeabilized membranes). After incubation of CTL with K<sup>d</sup>-PbCS(ABA) multimers, the annexin V staining increased 4.4-fold compared with untreated cells or cells incubated with noncognate K<sup>d</sup>-Cw3 170–179 multimers (Fig. 2 and data not shown). Essentially, the same

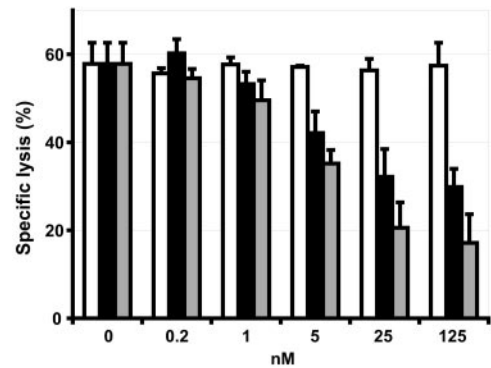
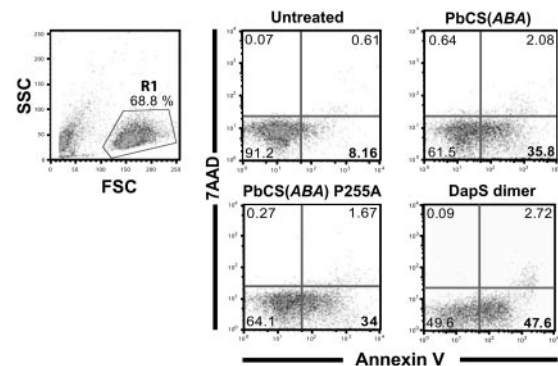


**FIGURE 1.** Soluble pMHC complexes inhibit target cell killing by S14 CTL. S14 CTL were incubated at 37°C for 30 min in the absence (□) or presence of indicated concentrations of K<sup>d</sup>-PbCS(ABA)P255A DapS dimer (■) or multimers (▒), and then added to <sup>51</sup>Cr-labeled P815 cells (E:T = 3:1) with 10 nM PbCS(ABA) peptide, and a standard cytotoxic assay was performed. The specific lysis was calculated from released chromium. Mean values and SD were calculated from three experiments.

results were obtained when K<sup>d</sup>-PbCS(ABA)P255A multimers were used, indicating that complexes containing the wild-type agonist (PbCS(ABA)) or the strong agonist (PbCS(ABA)P255A) were equally active. When cells were incubated with K<sup>d</sup>-PbCS(ABA)P255A DapS dimer, ~50% of the cells were annexin V positive. The fraction of 7AAD-positive cells increased in parallel with the annexin V-positive cells. After 30 min of incubation, this increase was ~3-fold, but then rapidly increased with the time of incubation (Fig. 2 and data not shown). Taken collectively, these results indicate that DapS dimer and multimers inhibit S14 CTL-mediated cytotoxicity by killing the CTL.

### Soluble pMHC complexes containing short linkers cause rapid death of cloned S14 CTL

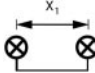
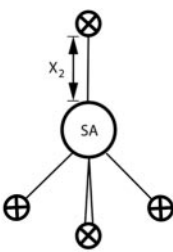
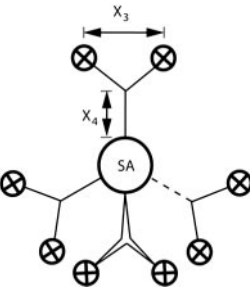
To extend the finding that pMHC dimers and multimers kill S14 CTL (Fig. 2), we tested additional well-defined soluble K<sup>d</sup>-PbCS(ABA)P255A complexes (Table I) for their ability to induce PS externalization. After 30 min of incubation with the short DapS dimer, ~50% of S14 CTL were annexin V positive, but upon



**FIGURE 2.** pMHC dimers and multimers rapidly induce PS externalization on cloned S14 CTL. S14 CTL were incubated at 37°C for 30 min in the absence (Untreated) or presence of 2 nM K<sup>d</sup> multimers containing the wild-type PbCS(ABA) peptide, the strong agonist variant PbCS(ABA)P255A, or K<sup>d</sup>-PbCS(ABA)P255A DapS dimer. Externalization of PS (dying cells) and membrane permeabilization (dead cells) were enumerated by staining with annexin V and 7AAD, respectively, and flow cytometry. Numbers indicate the fraction of cells in the given quadrants. One representative experiment of three is shown. FSC, Forward scatter; SSC, side scatter.



Table I. *The pMHC complexes under study*

pMHC Complexes		Linkers	Maximal Distance (Å)
Dimers 	DapS	Mal-Dap-(S <sup>c</sup> -Mal)-YDK (Cy5)-P	17.8 ( $x_1$ )
	P <sub>30</sub>	Cy5-Dap (Mal)-P <sub>30</sub> -Dap (Mal)-P	117 ( $x_1$ )
Tetramers 	PEO	I-CH <sub>2</sub> CO-NH-(PEO)-(CH <sub>2</sub> ) <sub>2</sub> -NH <sub>2</sub> -biotin	25 ( $x_2$ )
	P <sub>24</sub>	Biotin-Y-P <sub>24</sub> -K (Mal)-P	88 ( $x_2$ )
Octamer 	DapS/P <sub>10</sub>	$\begin{matrix} Mal-S \\ Mal-S \end{matrix} \rangle Dap-Y-P_{10}-K (biot)-P$	17.8/45 ( $x_3/x_4$ )

<sup>a</sup> Single-letter amino acid code is used.

incubation with the long P30 dimer, only 15% were (Fig. 3A). Following incubation with the PEO tetramer, approximately one-third of the cells externalized PS, i.e., slightly more compared with multimers. Conversely, the multimer containing the charge inversion D227K, which strongly reduces coengagement of CD8, induced only modest PS externalization, even though its binding to S14 CTL was only slightly reduced (Fig. 3, A and D). Upon incubation with DapS/P10 octamer, nearly one-half of the cells were annexin V positive. In all cases, no higher values were observed when higher pMHC concentrations were used (data not shown).

The PS externalization on S14 CTL increased with the concentration of the DapS dimer, reaching a maximum at 12.5–25 nM. The increase in intracellular calcium induced by DapS dimer exhibited essentially the same concentration dependence as the PS externalization (Fig. 3B). The same was true for the other pMHC complexes tested (data not shown). The pMHC concentrations giving maximal calcium mobilization and PS externalization were significantly lower than the concentrations giving maximal pMHC binding (Fig. 3, D–F). This difference was especially striking for the larger complexes (octamer > multimer > tetramer). Thus, the relatively small differences in binding between the long and short dimers and tetramers, and wild-type and D227K multimers, respectively, do not account for the observed large differences in biological activity. These experiments also show that the binding of the noncognate pMHC complexes to S14 CTL is very low; therefore, noncognate pMHC binding to CD8 is irrelevant for CTL activation in this system. The good temporal and dose-dependent correlation between PS externalization and CTL activation argues that these two processes are linked. In agreement with this, we found that monomers were unable to elicit PS externalization and

equally failed to activate S14 CTL (Fig. 3C and Ref. 29). This also shows that peptide transfer from soluble to cell-associated pMHC molecules (13, 14) does not account for the observed effects.

The PS externalization induced by DapS dimer was rapid, reaching a maximum after 30 min of incubation (Fig. 3C). However, this is likely to be an underestimate, because the number of dead cells (7AAD positive) increases with time and hence are not monitored in our flow cytometric assay (Fig. 2). To test this directly, we examined S14 CTL after different periods of incubation with DapS dimer by transmission and confocal microscopy. In a matter of a few minutes, the cells typically rounded up, and pronounced bleb formation and ballooning were observed (Fig. 4A). Already after 10 min, cells were damaged irreversibly, showing that PS externalization assessed by annexin V staining indeed reflects cell death. Also, S14 CTL rapidly exhibited strong clustering upon incubation with DapS dimer, which is typical for dying cells (Fig. 4B). The number of living cells steadily decreased over time, and after 1 h of incubation, cell debris and dead cells were abundant.

#### *Mechanism of DapS dimer-induced death of S14 CTL*

Because the previously described apoptosis of CTL by Fas-dependent mechanisms or fratricide typically occur with a slower kinetics than the rapid death observed here (Figs. 2 and 4; Refs. 10 and 12), we further explored the underlying mechanism. To this end, we tested the effects of inhibitors for perforin (concanamycin A), granzymes (zAADcmk), or caspases (zVADfmk) on DapS dimer-induced death of S14 CTL. None of these inhibitors had any effect (Fig. 5A), although, as expected, they inhibited to different degrees the lysis of sensitized target cells (B). Similar results were obtained for PEO tetramer and DapS/P10 octamer (data not shown).

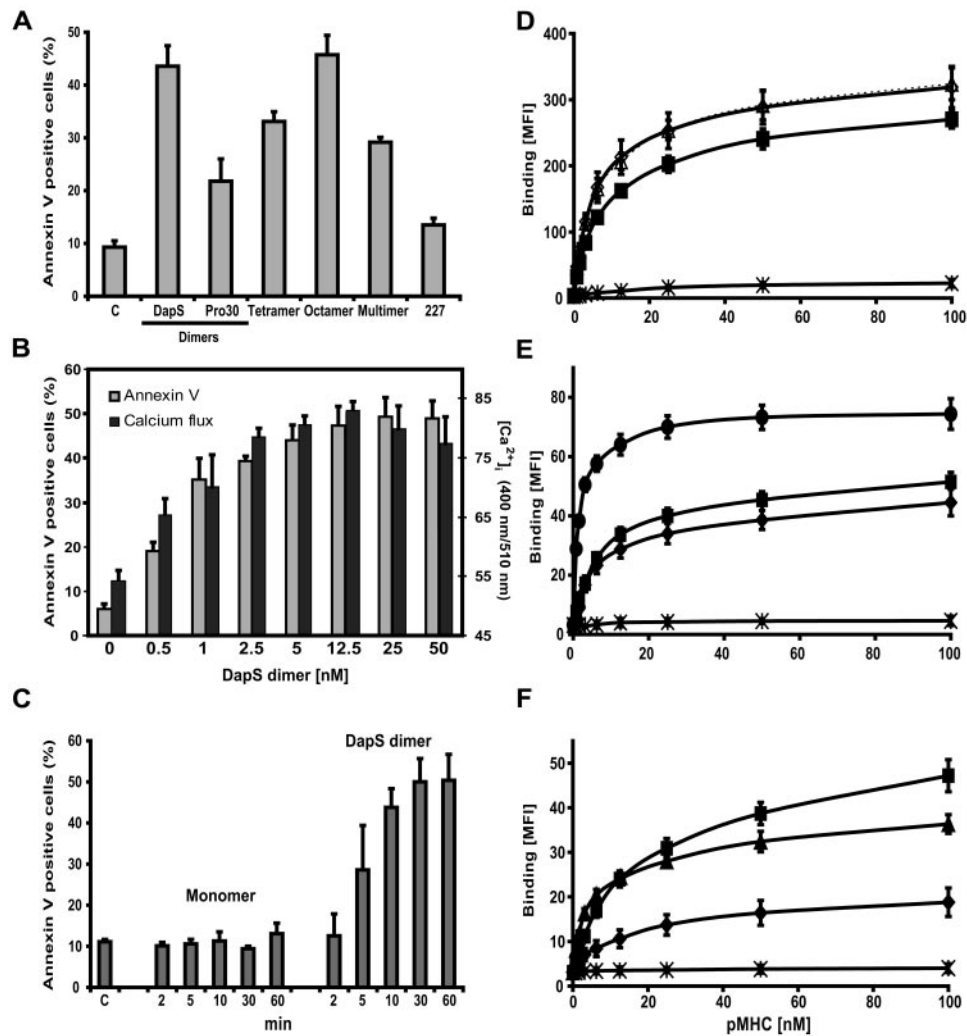


**FIGURE 3.** S14 CTL rapidly externalize PS after the activation with various soluble pMHC molecules. *A*, S14 CTL were incubated with K<sup>d</sup>-PbCS(ABA)P255A DapS dimer (12.5 nM), P30 dimer (12.5 nM), PEO tetramer (5 nM), DapS/P10 octamer (1 nM), multimers (2 nM), or K<sup>d</sup>D227K-PbCS(ABA)P255A multimers (4 nM) for 30 min at 37°C, and the percentage of annexin V-positive and 7AAD-negative cells was assessed by flow cytometry. The control (C) refers to untreated S14 CTL. SD were calculated from two independent experiments. *B*, S14 CTL were incubated likewise with the indicated concentrations of DapS dimer, and the percentage of annexin V-positive cells was assessed by flow cytometry (□). Alternatively, Indo-1-labeled S14 CTL were incubated with the same concentration of DapS dimer and calcium-dependent Indo-1 fluorescence was measured by flow cytometry over 3 min. ■, The maximal calcium responses. One representative of three experiments is shown. *C*, S14 CTL were incubated at 37°C for the indicated periods of time with monomer (200 nM) or DapS dimer (12.5 nM), and the percentage of annexin V-positive cells was assessed by flow cytometry. The control (C) refers to untreated S14 CTL. Mean values and SD were calculated from three experiments. *D–F*, S14 CTL were incubated at 37°C for 5 min with graded concentrations of the following: *D*, PE-labeled multimers containing the K<sup>d</sup>-PbCS(ABA) (◇), K<sup>d</sup>-PbCS(ABA)P255A (dashed line; △), K<sup>d</sup>D227K-PbCS(ABA) (■), or K<sup>d</sup>-Cw3 (170–179) (\*); *E*, Cy5-labeled K<sup>d</sup>-PbCS(ABA)P255A P24 tetramer (◆), PEO tetramer (■), DapS/P10 octamer (●), or DapS/P10 octamer containing the Cw3 peptide 170–179 (\*); or *F*, Cy5-labeled K<sup>d</sup>-PbCS(ABA)P255A monomer (◆), DapS dimer (■), P30 dimer (▲), or DapS dimer containing the Cw3 170–179 peptide (\*), and cell-associated fluorescence was measured by flow cytometry after UV irradiation and washing. Mean values and SD were calculated from two to four experiments. Of note, the molar fluorescent intensities are the same for the multimers, the tetramers and octamers, and the monomer and dimers, respectively.

Testing of additional inhibitors showed that the DapS dimer-induced death of S14 CTL was inhibited by agents that impede CTL activation, such as inhibitors for protein kinase C (PKC), PI3K, MAPK and Src kinases, the cation chelator EDTA, and the actin polymerization inhibitor latrunculin A (Table II). By contrast, blocking of CD28, CTLA-4, or protein synthesis had no effect.

We next investigated whether DapS dimer triggers S14 CTL by bystander cell killing. Significant lysis of unsensitized P815 cells was observed only at high concentrations of DapS dimer and only in the absence of brefeldin A (Fig. 5C). Brefeldin A blocks the transfer of exogenous peptides to cell-associated MHC molecules and has no effect on target cell killing, arguing that this bystander

cell killing is accounted for by transfer of peptide from soluble to cell-associated MHC molecules (Refs. 13, 14, and 30, and data not shown). To prevent such peptide transfer and thus to rule out fratricide of CTL, brefeldin A was included in all experiments. Finally, the DapS dimer-induced death of S14 CTL was not affected by the soluble death receptors Fas, TNFR1, and TRAILR2, which in control experiments completely inhibited Fas ligand-, TNF- $\alpha$ -, and TRAIL-mediated cytotoxicity (Fig. 5D; Refs. 26 and 27; data not shown). Taken together, these results indicate that pMHC-induced death of S14 CTL requires full CTL activation, but is not mediated by perforin/granzymes, fratricide, nor classical death receptors.

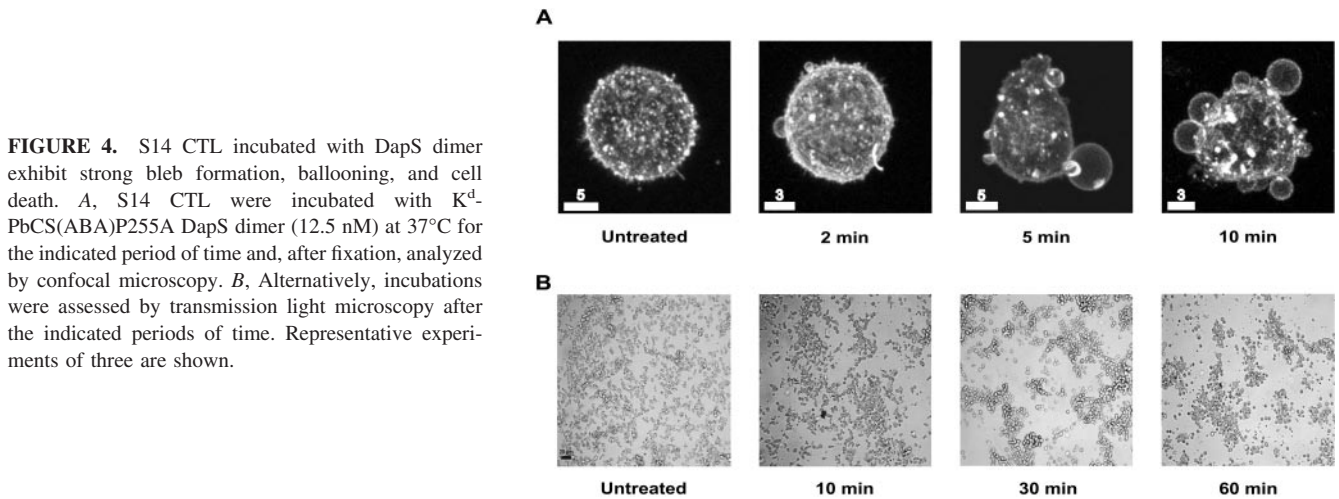


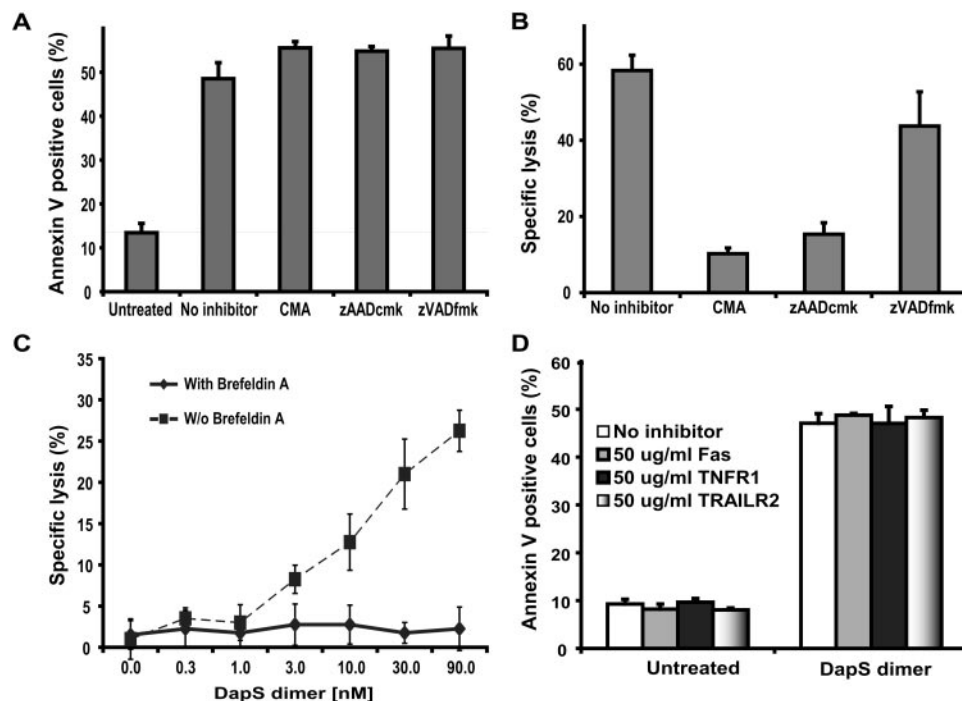
**FIGURE 4.** S14 CTL incubated with DapS dimer exhibit strong bleb formation, ballooning, and cell death. *A*, S14 CTL were incubated with K<sup>d</sup>-PbCS(ABA)P255A DapS dimer (12.5 nM) at 37°C for the indicated period of time and, after fixation, analyzed by confocal microscopy. *B*, Alternatively, incubations were assessed by transmission light microscopy after the indicated periods of time. Representative experiments of three are shown.

*Soluble pMHC complexes trigger depolarization of mitochondrial membranes and production of ROS*

To assess whether pMHC complex-induced cell death relies on mitochondrial dysfunction, we examined what effect different K<sup>d</sup>-PbCS(ABA)P255A complexes have on  $\Delta\psi_m$  on S14 CTL. To this end, the cells were incubated with pMHC complexes and TMRM, which binds to polarized, but not depolarized, mitochondrial membranes (31). S14 CTL upon incubation with short DapS dimer and DapS/P10 octamer exhibited substantially less TMRM fluorescence compared with untreated cells (Fig. 6A). CTL incubated with monomeric or long P30 dimeric complexes exhibited only

slightly reduced TMRM fluorescence. Thus, in accordance with the annexin V staining, the short pMHC complexes caused loss of the  $\Delta\psi_m$ , which is a hallmark of mitochondrial dysfunction-mediated death (32). Essentially the same results were obtained when using DiOC<sub>6</sub>, another sensitive dye (Ref. 33 and data not shown).

When the CTL were incubated instead with DHR, which acquires fluorescence in the presence of ROS (34), the opposite situation was observed. Cells incubated with the short dimeric and octameric complexes exhibited strong DHR fluorescence compared with untreated cells or cells incubated with monomeric or long P30 dimeric complexes (Fig. 6B). Essentially, the same



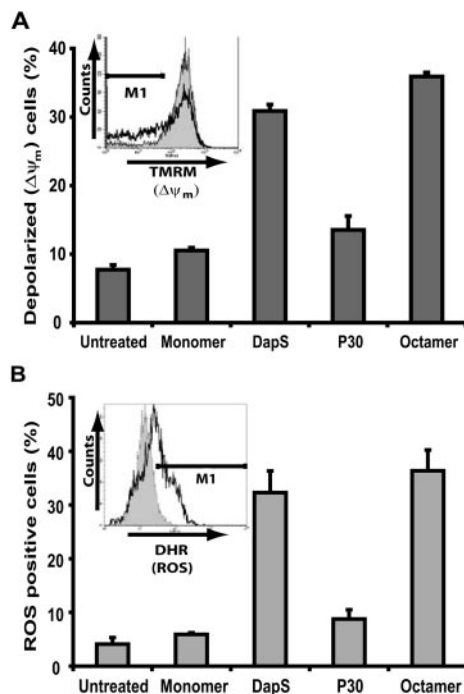
**FIGURE 5.** DapS dimer-induced death of S14 CTL does not rely on classical cell death pathways. *A*, S14 CTL untreated or preincubated with inhibitors for perforin (concanamycin A; CMA), granzymes (zAAD-cmk), or caspases (zVAD-fmk) were incubated at 37°C for 30 min with K<sup>d</sup>-PbCS(ABA)P255A DapS dimer (12.5 nM), and the percentage of annexin V-positive cells was assessed by flow cytometry. *B*, S14 CTL pretreated likewise were incubated for 4 h at 37°C with <sup>51</sup>Cr-labeled P815 cells (E:T = 3:1) previously pulsed with PbCS(ABA) peptide (1 nM). Specific lysis was calculated from released chromium. Mean values and SD were calculated from three experiments. *C*, S14 CTL, untreated (◆) or treated with 20 μM brefeldin A (■), were incubated with <sup>51</sup>Cr-labeled P815 cells, and specific lysis was assessed as described for *B*. *D*, S14 CTL were incubated with DapS dimer (12.5 nM) together with the indicated soluble death receptors (50 μg/ml) for 30 min at 37°C, and the percentage of annexin V cells was assessed by flow cytometry. Mean values and SD were calculated from two experiments.

Table II. The effect of inhibitors on death of S14 CTL induced by 12.5 nM DapS dimer for 30 min at 37°C<sup>a</sup>

Ab/Inhibitor/Agent	Affected/Inhibited Process	Inhibition of PS Externalization
Anti-CD28 Ab	Costimulation	—
Anti-CTLA-4 Ab	Costimulation	—
Concanamycin A	Perforin killing	—
zVADfmk	Pan-caspase	—
zAADcmk	Granzymes	—
zDEVDfmk	Caspase-3 specific	—
E64d	Cathepsin B and L	—
<b>PP2</b>	Src family kinases	++++
<b>Latrunculin A</b>	Actin polymerization	+++
<b>Wortmanin</b>	PI3K	+++
<b>Rottlerin</b>	Classical PKC	++++
<b>Gö6976</b>	Nonclassical PKC	++++
<b>SB202192</b>	p38 MAPK	++++
Cycloheximide	De novo protein synthesis	—
Sodium azide	ABC transporter inhibitor	—
<b>EDTA</b>	Chelating agent	++++

<sup>a</sup> Key: —, 0–5%; ++, 30–50%; +++, 50–80%; +++++, 80–100%. The inhibitors that negatively regulate signaling induced by TCR/CD8 coengagement are indicated in bold.

results were obtained when using hydroethidium, another ROS-sensitive dye (Ref. 33 and data not shown). These results indicate that soluble pMHC complexes, which cause the death of



**FIGURE 6.** DapS dimer induces mitochondrial membrane depolarization and ROS production in S14 CTL. *A*, S14 CTL were incubated for 30 min at 37°C with K<sup>d</sup>-PbCS(ABA)P255A monomer (200 nM), DapS dimer (12.5 nM), P30 dimer (12.5 nM), or DapS/P10 octamer (1 nM), and the Δψ<sub>m</sub>-dependent dye TMRM, and analyzed by flow cytometry. Bars represent the percentage of cells with depolarized mitochondria. The inset demonstrates a representative histogram of untreated (filled) and DapS dimer-treated (bold line) cells and the gate used for evaluation. *B*, S14 CTL were labeled with the ROS-sensitive dye DHR, treated with the different pMHC complexes as described for *A*, and ROS-dependent increase of DHR fluorescence was measured by flow cytometry. Bars represent the percentage of cells with increased ROS. The inset shows a representative histogram of untreated (filled), respectively DapS dimer-treated (bold line) S14 CTL, and the gate used for evaluation. Mean values and SD were calculated from three experiments.

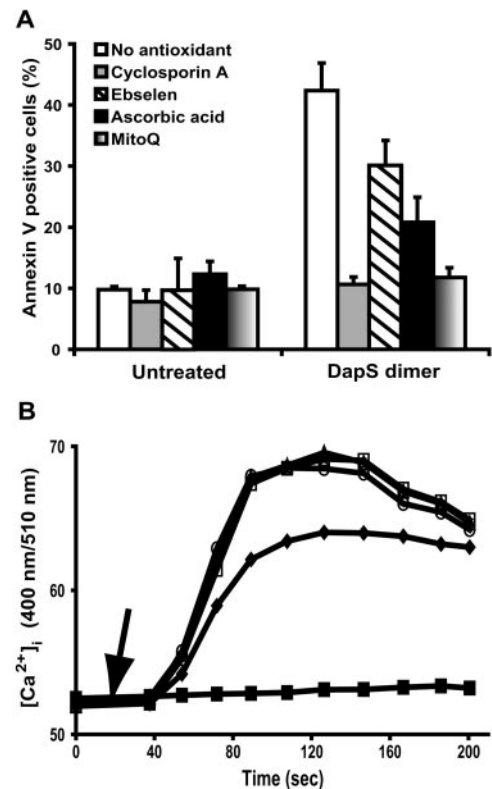


**FIGURE 7.** Inhibitory effect of antioxidants and cyclosporin A on soluble pMHC-induced S14 CTL death. *A*, S14 CTL, untreated or pretreated with cyclosporin A (25 μM) and the antioxidants ebselen (20 μM), vitamin C (1 mg/ml), or MitoQ (1 μM), respectively, were incubated at 37°C for 30 min with K<sup>d</sup>-PbCS(ABA)P255A DapS dimer (12.5 nM), and the percentage of annexin V-positive cells was assessed by flow cytometry. Mean values and SD were calculated from two experiments. *B*, S14 CTL, untreated (Δ) or pretreated with ebselen (○), vitamin C (□) and cyclosporin A (◆), respectively, were labeled with Indo-1, and its calcium-dependent fluorescence was analyzed for 3 min after stimulation with 12.5 nM DapS dimers. Untreated and unstimulated cells (■) were used as control. The arrow indicates the addition of DapS dimer.

S14 CTL, also induce depolarization of mitochondrial membranes and generation of ROS. This is in accordance with studies showing that depolarization of mitochondrial membranes and generation of ROS leads to mitochondrial dysfunction and T cell death (5, 32).

#### Antioxidants and cyclosporin A inhibit pMHC-induced CTL death

Because of the known relationship between ROS generation and mitochondrial dysfunction (32), we tested several antioxidants known to inhibit ROS production. MitoQ, a mitochondria-targeted antioxidant (35), completely inhibited the DapS dimer-induced death of S14 CTL (Fig. 7*A*). In addition, vitamin C strongly inhibited S14 CTL PS externalization, whereas ebselen only moderately. At the concentrations used, these antioxidants were not toxic and had no effect on the intracellular calcium mobilization induced by DapS dimer (Fig. 7*B*). For MitoQ, calcium measurements were not performed, because its fluorescence overlaps with that of Indo-1. The superoxide dismutase mimetic, Mn(III)tetrakis(5,10,15,20-benzoic acid)porphyrin (200 μM MnTBAP), also inhibited DapS dimer-induced PS externalization; however, at the concentrations required, it also inhibited calcium mobilization and tyrosine phosphorylation (data not shown). Cyclosporin A completely inhibited PS externalization,



but moderately also inhibited the DapS dimer-induced calcium mobilization.

#### Soluble pMHC complexes induce necrosis rather than apoptosis of S14 CTL

A hallmark of Fas-mediated apoptosis of T cells is DNA fragmentation and release of cytochrome *c* from mitochondria into the cytosol. As assessed by the TUNEL assay, S14 CTL exhibited only modest DNA fragmentation upon incubation with DapS dimer in the assayed 30-min period (Fig. 8A). After 30 min of incubation, no cytochrome *c* was detectable in the cytosol (Fig. 8B). The conclusion that therefore DapS dimer-induced death of S14 CTL is not apoptosis is supported by electron microscopy. S14 CTL incubated with DapS dimer exhibited nonapoptotic nuclei (dispersed foci of chromatin and heterochromatin), nonhomogeneous cytoplasmic pattern, rounded mitochondria with disrupted internal structures, and extensive vacuolization compared with the untreated cells (Fig. 9). In particular, the vacuolation of the cytoplasm, rounding of mitochondria, and disruption of their internal structures are characteristic for programmed necrosis but not for apoptosis (36).

#### Short but not long pMHC complexes efficiently kill effector but not naive CD8<sup>+</sup> T1 T cells

To determine the general relevance of the findings obtained using cloned S14 CTL, we examined T cells from primed T1 TCR transgenic mice. To this end, effector T1 T cells were incubated with

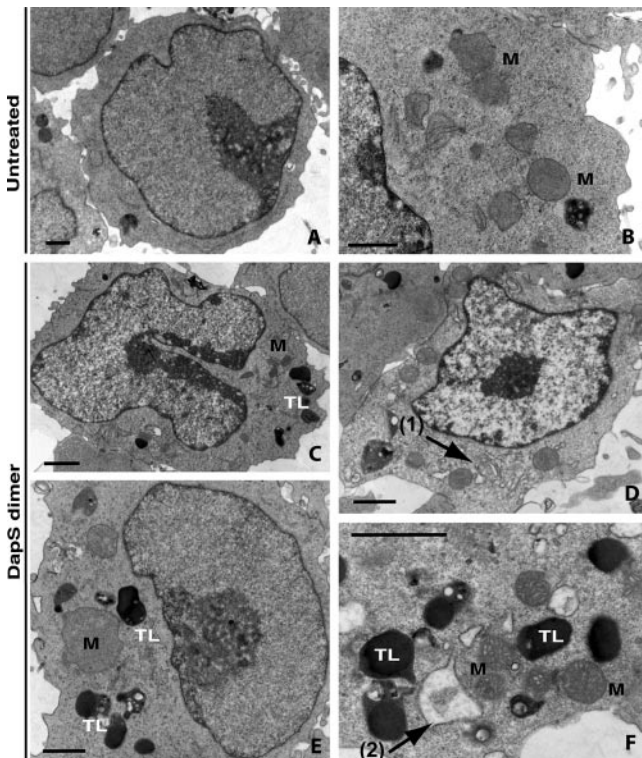


**FIGURE 9.** DapS dimer induces morphological changes in S14 CTL consistent with programmed necrosis. S14 CTL untreated (A and B) or upon incubation with K<sup>d</sup>-PbCS(ABA)P255A DapS dimer for 15 min at 37°C (12.5 nM) (C–F) were fixed and analyzed by transmission electron microscopy. Unlike untreated cells, CTL incubated with DapS dimer exhibited depletion of chromatin density and chromatin clumping (C and D), appearance of multiple dense large telolysosomes (TL), dilated endoplasmic reticulum (arrow 1) and Golgi apparatus (arrow 2), altered mitochondria (M) of irregular and dilated shape (E) or with condensed matrix (F). Bars represent 1  $\mu$ m.

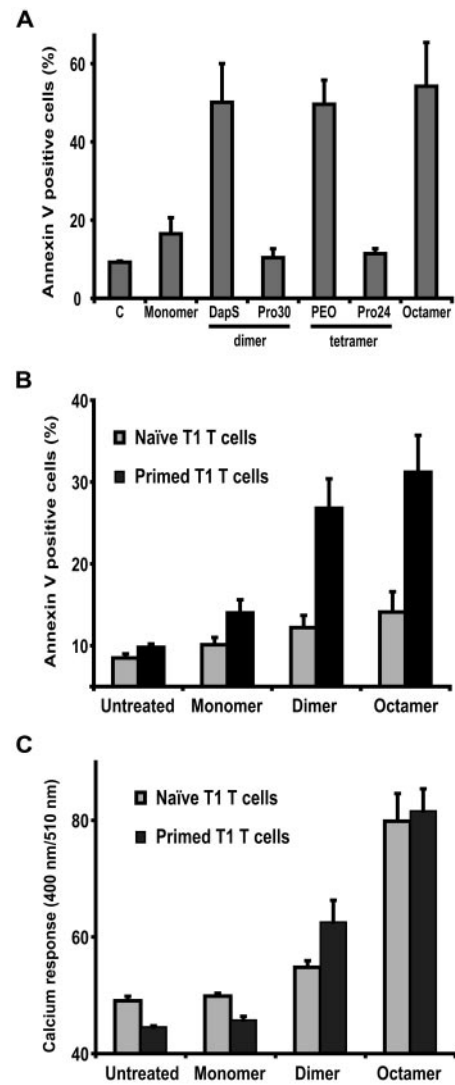


**FIGURE 10.** Primed T1 T cells are more susceptible to soluble pMHC-induced death than naive cells. A, Effector T cells from T1 TCR Tg RAG-2<sup>-/-</sup> mice were incubated at 37°C for 30 min with K<sup>d</sup>-PbCS(ABA)P255L monomer (100 nM), DapS dimer (12.5 nM), P30 dimer (12.5 nM), PEO tetramer (5 nM), P24 tetramer (5 nM), or DapS/P10 octamer (1 nM), and the percentage of Cy5-labeled annexin V-positive cells was analyzed by flow cytometry. B, Naive (□) and effector (■) T1 T cells were incubated likewise with monomer (100 nM), DapS dimer (12.5 nM), or DapS/P10 octamer (1 nM), and the percentage of FITC-labeled annexin V-positive cells was determined by flow cytometry. C, Indo-1-labeled naive (□) and effector (■) T1 T cells were incubated at 37°C with monomers (100 nM), DapS dimer (12.5 nM), or DapS/P10 octamer (1 nM), and calcium-dependent fluorescence was analyzed by flow cytometry for 3 min. Maximal calcium responses are shown. Mean values and SD were calculated from three experiments.

K<sup>d</sup>-PbCS(ABA)P255L monomer, DapS and P30 dimers, PEO and P24 tetramers, or DapS/P10 octamer, and PS externalization was analyzed by flow cytometry. In good agreement with the results obtained on S14 CTL, DapS dimer, PEO tetramer, and DapS/P10 octamer induced extensive PS externalization (Fig. 10A). By contrast, the monomer as well as the long P30 dimer and P24 tetramer gave only modest or background levels. No higher values were observed when higher pMHC concentrations were used.

Effector T1 T cells, upon incubation with DapS dimer and DapS/P10 octamer, exhibited much stronger annexin V staining



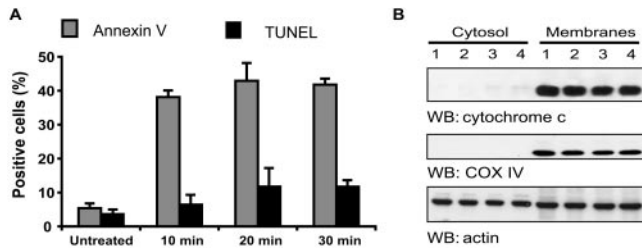


**FIGURE 8.** DapS dimer-induced S14 CTL death is not accompanied by cytochrome *c* release and DNA fragmentation. *A*, S14 CTL were incubated at 37°C for the indicated periods of time with K<sup>4</sup>-PbCS(ABA)P255A DapS dimer (12.5 nM), and DNA fragmentation was assessed by flow cytometry upon labeling of DNA fragments (TUNEL) (■). Alternatively, cells were stained with annexin V and analyzed by flow cytometry (▣). Mean values and SD were calculated from two independent experiments. *B*, Untreated S14 CTL (lane 1) or cells incubated at 37°C for 30 min with monomer (200 nM) (lane 2), DapS dimer (12.5 nM) (lane 3), or P30 dimer (12.5 nM) (lane 4) were lysed on ice with digitonin. Detergent-soluble (Cytosol) and -insoluble membrane fractions (Membranes) were resolved on SDS-PAGE and Western blotted with Abs specific for cytochrome *c*, COX IV, and actin, respectively. One representative of two experiments is shown.

compared with naive T1 T cells (Fig. 10*B*). By contrast, the calcium responses induced by these complexes were similar on naive and activated T1 T cells (Fig. 10*C*), arguing that the resistance of the naive T1 T cells to undergo pMHC complex-induced death is not explained by lack of cell activation. As on S14 CTL, the concentrations giving maximal biological activity were significantly below those giving maximal binding (data not shown). Taken together, these findings indicate that effector, but not naive T1 T cells, like cloned S14 CTL, are susceptible to pMHC complex-induced, activation-dependent death. By examining the susceptibility of T1 T cells to undergo pMHC-induced death at different stages of differentiation, we found that it correlates with their acquisition of cytotoxicity (data not shown).

## Discussion

The key finding of the present study is that activated effector CTL undergo rapid cell death upon exposure to soluble pMHC complexes. The cell death described here is clearly different from the previously described pMHC-induced apoptosis of CTL (10, 12). First, it occurs with a much faster kinetics. Although Fas-dependent death of CTL was extensive only after several hours of incubation with pMHC, the death described here is induced within a few minutes (12, 37). This does not exclude that CTL that resist the rapid pMHC-induced death described here succumb at a later time to Fas-dependent apoptosis. It is important to note, however, that upon prolonged incubation of CTL with soluble pMHC complexes, transfer of peptide from soluble to cell-associated MHC molecules does occur (13, 14). Although we show here that brefeldin A impedes this peptide transfer, mainly by inhibiting loading of newly synthesized MHC molecules (30), this inhibition is effective only for a limited time (Fig. 5*C* and our unpublished results).

Second, the CTL death described here requires CD8 coengagement and full CTL activation, whereas Fas-dependent CTL death can occur without CD8 coengagement and extensive CTL activation (12). Third, although binding of death ligands to their respective death receptors, Fas, TNFR1, and TRAILR2, as well as activation of caspases play a crucial role in T cell apoptosis (38), none of this was observed for the pMHC-induced CTL death described here (Fig. 5). Fourth, a hallmark of classical apoptosis is cytochrome release from mitochondria into the cytosol, DNA fragmen-

tation, and strong chromatin condensation (15, 36, 38). Neither cytochrome *c* release nor marked DNA fragmentation and chromatin condensation were observed in DapS dimer-treated S14 CTL (Figs. 8 and 9). Instead, CTL incubated with DapS dimer exhibited inhomogeneous cytoplasmic pattern with strong vacuolization, rounded mitochondria with disrupted internal structures, which are characteristic for programmed necrosis (36, 38). The rapid formation of blebs and ballooning observed on pMHC-pulsed CTL together with extensive vacuolization of the cytoplasm are also typical for autophagy (36, 39), indicating that the pMHC-induced CTL death harbors features both of programmed necrosis and autophagy.

As has been described for programmed necrosis, the pMHC-induced CTL death involves the generation of ROS and depolarization of mitochondrial membranes, which results in lethal mitochondrial dysfunction (32). In agreement with this, we found that cyclosporin A, which putatively protects mitochondria by inhibiting permeability transition pore opening (40), prevents pMHC-induced death of CTL (Fig. 7). However, it should be noted that cyclosporin A also inhibits the protein phosphatase calcineurin, which is involved in T cell signaling (41). A likely scenario is that pMHC complexes containing short linkers (i.e., DapS dimer and DapS/P10 octamer) strongly activate CTL, and therefore trigger high mitochondrial activity to meet the increased demand of ATP (42). The observed production of ROS thus probably results from interaction of electrons shed from the respiratory chain with molecular oxygen, resulting in formation of superoxide and by catalytic conversion in other ROS (32, 42). The production of ROS and depolarization of mitochondrial membranes and the ensuing mitochondrial dysfunction are linked, as seen by the inhibition of pMHC-induced cell death by antioxidants, in particular of MitoQ, which selectively targets mitochondria (35).

The failure of the long pMHC complexes to elicit death of CTL thus is best explained by their inability to activate CTL. The short DapS, but not the long P30 dimer induced strong calcium mobilization and phosphorylation of signaling molecules (e.g., Lck, linker for activation of T cells (LAT), ZAP-70, and phospholipase C $\gamma$ 1) (21). Similar differences were observed for the long and short tetramers (our unpublished results). The most plausible explanation for this is that the short pMHC oligomers induce strong co-cross-linking of TCR and CD8, resulting in vigorous activation of Src kinases, namely, CD8-associated Lck, which is the initial critical event in pMHC-driven CTL activation (10, 12, 29). In accordance with this is the finding that monomeric and pMHC complexes containing long rigid spacers elicit no or scant CTL activation and CTL death (Figs. 3, 4, and 10; Ref. 21 and our unpublished data). Also, inhibition of CTL activation by different agents impaired pMHC-mediated CTL death (Table II).

Other factors that determine the susceptibility of T cells to undergo pMHC activation-dependent autonomous death is the expression of anti- and proapoptotic Bcl-2 family members such as Bcl-2, Bcl-x<sub>L</sub>, Bax, Bim, and Bcl-2/adenovirus E1B 19-kDa protein-interacting protein 3 (BNIP3) (6, 43). As assessed by Western blotting, both S14 TCR and effector T1 T cells expressed high levels of the latter two molecules (our unpublished results). Although Bcl-2 prevents T cell death, Bim and BNIP3 promote it, namely, by acting at the mitochondrial outer membrane (6, 43). Bim, but not BNIP3, was reported to induce the activation of effector caspases and cytochrome *c* release from mitochondria (5, 44, 45). The relative expression levels of Bcl-2 anti- and proapoptotic family members thus determine the susceptibility of T cells to undergo mitochondrial dysfunction-mediated cell death. Because

naïve and memory T cells typically express higher levels of anti-apoptotic molecules, namely, Bcl-2, than activated effector CTL, this most likely explains why the latter are more susceptible to pMHC-induced death (6, 46).

Although it is established that expression of Bcl-2 and its family members in T cells is dependent on their differentiation and state of activation (46), it seems also to be a clonal property. In a currently ongoing study, we have found that HLA-A2-restricted Melan A-specific CTL clones obtained by FACS cloning with reversible tetramers, exhibit different susceptibility to undergo pMHC activation-dependent death. It is therefore conceivable that, upon FACS sorting or cloning using conventional pMHC multimers, certain CTL are selectively lost. This is intriguing in view of the observation that Melan A-specific CTL that were cloned by using CD8 binding-deficient pMHC multimers, more effectively killed melanoma cells when compared with CTL obtained by cloning using conventional multimers (47). Also, CTL that were obtained by FACS cloning using reversible multimers exhibited superior lytic properties than CTL isolated by means of conventional multimers (11). Both the CD8 binding-deficient and the reversible pMHC multimers have greatly reduced ability to activate Ag-specific CTL (11, 48). In view of our finding that pMHC-provoked death of CTL is activation dependent (Fig. 3 and Table I), this probably explains why these reagents allow isolation of bona fide CTL.

In the present study, we show for the first time that the soluble pMHC complexes' induced death of CTL depends on their ability to activate the CTL (Fig. 3; Table I). The key determinant for this is the distance between individual pMHC units and to a much lesser extent their valence, which largely determines their ability to activate CTL. This is illustrated by the dimeric pMHC complexes. Dimers containing short linkers strongly trigger calcium mobilization, diverse phosphorylation events, and CTL death, whereas dimers containing long linkers do not (Figs. 2–4 and 10; Ref. 21). The same was true for tetramers: those containing the short PEO linker (25 Å) induced strong calcium mobilization and CTL death, whereas those containing the long P24 linker (88 Å) were inactive (Figs. 3 and 10, and our unpublished results). Thus, in terms of practical applications, soluble pMHC complexes containing short linkers can be used to eradicate Ag-specific CTL. This may be of interest in autoimmune disorders like diabetes type I, for which a growing number of epitopes of CTL involved in the disease induction are identified (49). In contrast, soluble complexes containing long linkers should be used when the aim is to isolate bona fide CTL. Because such complexes are inexpensive and simple to prepare, they therefore provide an attractive alternative to the reversible pMHC complexes.

## Acknowledgments

We are thankful to Margot Thome, Mike P. Murphy, and Ladislav Andera for helpful discussions. We also thank Ivana Novakova and Rolf Cornaz for technical assistance.

## Disclosures

The authors have no financial conflict of interest.

## References

- Gao, G. F., Z. Rao, and J. I. Bell. 2002. Molecular coordination of  $\alpha\beta$  T-cell receptors and co-receptors CD8 and CD4 in their recognition of peptide-MHC ligands. *Trends Immunol.* 23: 408–413.
- Siegel, R. M., F. K. Chan, H. J. Chun, and M. J. Lenardo. 2000. The multifaceted role of Fas signaling in immune cell homeostasis and autoimmunity. *Nat. Immunol.* 1: 469–474.
- Green, D. R., N. Droin, and M. Pinkoski. 2003. Activation-induced cell death in T cells. *Immunol. Rev.* 193: 70–81.
- Zheng, L., G. Fisher, R. E. Miller, J. Peschon, D. H. Lynch, and M. J. Lenardo. 1995. Induction of apoptosis in mature T cells by tumour necrosis factor. *Nature* 377: 348–351.
- Hildeman, D. A., Y. Zhu, T. C. Mitchell, P. Bouillet, A. Strasser, J. Kappler, and P. Marrack. 2002. Activated T cell death in vivo mediated by proapoptotic bcl-2 family member Bim. *Immunity* 16: 759–767.
- Tripathi, P., and D. Hildeman. 2004. Sensitization of T cells to apoptosis: a role for ROS? *Apoptosis* 9: 515–523.
- Hildeman, D. A., T. Mitchell, J. Kappler, and P. Marrack. 2003. T cell apoptosis and reactive oxygen species. *J. Clin. Invest.* 111: 575–581.
- Altman, J. D., P. A. H. Moss, P. J. R. Goulder, D. H. Barouch, M. G. McHeyzer-Williams, J. I. Bell, A. J. McMichael, and M. M. Davis. 1996. Phenotypic analysis of antigen-specific T lymphocytes. *Science* 274: 94–96.
- Schneck, J., W. L. Maloy, J. E. Coligan, and D. H. Margulies. 1989. Inhibition of an allospecific T cell hybridoma by soluble class I proteins and peptides: estimation of the affinity of a T cell receptor for MHC. *Cell* 56: 47–55.
- Guillaume, P., D. F. Legler, N. Boucheron, M. A. Doucey, J. C. Cerottini, and I. F. Luescher. 2003. Soluble major histocompatibility complex-peptide octamers with impaired CD8 binding selectively induce FAS-dependent apoptosis. *J. Biol. Chem.* 278: 4500–4509.
- Knabel, M., T. J. Franz, M. Schiemann, A. Wulf, B. Villmow, B. Schmidt, H. Bernhard, H. Wagner, and D. H. Busch. 2002. Reversible MHC multimer staining for functional isolation of T-cell populations and effective adoptive transfer. *Nat. Med.* 8: 631–637.
- Xu, X. N., M. A. Purbhoo, N. Chen, J. Mongkolsapaya, J. H. Cox, U. C. Meier, S. Tafuro, P. R. Dunbar, A. K. Sewell, C. S. Hourigan, et al. 2001. A novel approach to antigen-specific deletion of CTL with minimal cellular activation using  $\alpha 3$  domain mutants of MHC class I/peptide complex. *Immunity* 14: 591–602.
- Ge, Q., J. D. Stone, M. T. Thompson, J. R. Cochran, M. Rushe, H. N. Eisen, J. Chen, and L. J. Stern. 2002. Soluble peptide-MHC monomers cause activation of CD8<sup>+</sup> T cells through transfer of the peptide to T cell MHC molecules. *Proc. Natl. Acad. Sci. USA* 99: 13729–13734.
- Schott, E., N. Bertho, Q. Ge, M. M. Maurice, and H. L. Ploegh. 2002. Class I negative CD8 T cells reveal the confounding role of peptide-transfer onto CD8 T cells stimulated with soluble H2-K<sup>b</sup> molecules. *Proc. Natl. Acad. Sci. USA* 99: 13735–13740.
- Takahashi, M., E. Osono, Y. Nakagawa, J. Wang, J. A. Berzofsky, D. H. Margulies, and H. Takahashi. 2002. Rapid induction of apoptosis in CD8<sup>+</sup> HIV-1 envelope-specific murine CTLs by short exposure to antigenic peptide. *J. Immunol.* 169: 6588–6593.
- Masteller, E. L., M. R. Warner, W. Ferlin, V. Judkowski, D. Wilson, N. Glaichenhaus, and J. A. Bluestone. 2003. Peptide-MHC class II dimers as therapeutics to modulate antigen-specific T cell responses in autoimmune diabetes. *J. Immunol.* 171: 5587–5595.
- Casares, S., A. Hurtado, R. C. McEvoy, A. Sarukhan, H. von Boehmer, and T. D. Brumeanu. 2002. Down-regulation of diabetogenic CD4<sup>+</sup> T cells by a soluble dimeric peptide-MHC class II chimera. *Nat. Immunol.* 3: 383–391.
- Burrows, G. G., K. L. Adlard, B. F. Bebo, Jr., J. W. Chang, K. Tenditnyy, A. A. Vandenbark, and H. Offner. 2000. Regulation of encephalitogenic T cells with recombinant TCR ligands. *J. Immunol.* 164: 6366–6371.
- O'Herrin, S. M., J. E. Slansky, Q. Tang, M. A. Markiewicz, T. F. Gajewski, D. M. Pardoll, J. P. Schneck, and J. A. Bluestone. 2001. Antigen-specific blockade of T cells in vivo using dimeric MHC peptide. *J. Immunol.* 167: 2555–2560.
- Dal Porto, J., T. E. Johansen, B. Catipovic, D. J. Parfiit, D. Tuveson, U. Gether, S. Kozlowski, D. T. Fearon, and J. P. Schneck. 1993. A soluble divalent class I major histocompatibility complex molecule inhibits alloreactive T cells at nanomolar concentrations. *Proc. Natl. Acad. Sci. USA* 90: 6671–6675.
- Cebecauer, M., P. Guillaume, S. Mark, O. Michielin, N. Boucheron, M. Bezard, B. H. Meyer, J.-M. Segura, H. Vogel, and I. F. Luescher. CD8<sup>+</sup> cytotoxic T lymphocyte activation by soluble major histocompatibility complex (MHC)-peptide dimers. *J. Biol. Chem. In press.*
- Arora, P. S., A. Z. Ansari, T. P. Best, M. Ptashne, and P. B. Dervan. 2002. Design of artificial transcriptional activators with rigid poly-L-proline linkers. *J. Am. Chem. Soc.* 124: 13067–13071.
- Luescher, I. F., F. Anjuere, M. C. Peitsch, C. V. Jongeneel, J. C. Cerottini, and P. Romero. 1995. Structural analysis of TCR-ligand interactions studied on H-2K<sup>d</sup>-restricted cloned CTL specific for a photoreactive peptide derivative. *Immunity* 3: 51–63.
- Holler, N., T. Kataoka, J. L. Bodmer, P. Romero, J. Romero, D. Deperthes, J. Engel, J. Tschopp, and P. Schneider. 2000. Development of improved soluble inhibitors of FasL and CD40L based on oligomerized receptors. *J. Immunol. Methods* 237: 159–173.
- Schneider, P. 2000. Production of recombinant TRAIL and TRAIL receptor: Fc chimeric proteins. *Methods Enzymol.* 322: 325–345.
- Doucey, M. A., D. F. Legler, M. Faroudi, N. Boucheron, P. Baumgaertner, D. Naecher, M. Cebecauer, D. Hudrisier, C. Ruegg, E. Palmer, et al. 2003. The  $\beta_1$  and  $\beta_3$  integrins promote T cell receptor-mediated cytotoxic T lymphocyte activation. *J. Biol. Chem.* 278: 26983–26991.

29. Doucey, M. A., D. F. Legler, N. Boucheron, J. C. Cerottini, C. Bron, and I. F. Luescher. 2001. CTL activation is induced by cross-linking of TCR/MHC-peptide-CD8/p56<sup>lck</sup> adducts in rafts. *Eur. J. Immunol.* 31: 1561–1570.
30. Luescher, I. F., P. Romero, J. C. Cerottini, and J. L. Maryanski. 1991. Specific binding of antigenic peptides to cell-associated MHC class I molecules. *Nature* 351: 72–74.
31. Rasola, A., and M. Geuna. 2001. A flow cytometry assay simultaneously detects independent apoptotic parameters. *Cytometry* 45: 151–157.
32. Perl, A., P. Gergely, Jr., G. Nagy, A. Koncz, and K. Banki. 2004. Mitochondrial hyperpolarization: a checkpoint of T-cell life, death and autoimmunity. *Trends Immunol.* 25: 360–367.
33. Grayson, J. M., N. G. Laniewski, J. G. Lanier, and R. Ahmed. 2003. Mitochondrial potential and reactive oxygen intermediates in antigen-specific CD8<sup>+</sup> T cells during viral infection. *J. Immunol.* 170: 4745–4751.
34. Frey, T. 1997. Correlated flow cytometric analysis of terminal events in apoptosis reveals the absence of some changes in some model systems. *Cytometry* 28: 253–263.
35. Kelso, G. F., C. M. Porteous, C. V. Coulter, G. Hughes, W. K. Porteous, E. C. Ledgerwood, R. A. J. Smith, and M. P. Murphy. 2001. Selective targeting of a redox-active ubiquinone to mitochondria within cells: antioxidant and anti-apoptotic properties. *J. Biol. Chem.* 276: 4588–4596.
36. Edinger, A. L., and C. B. Thompson. 2004. Death by design: apoptosis, necrosis and autophagy. *Curr. Opin. Cell Biol.* 16: 663–669.
37. Van Parijs, L., A. Biuckians, and A. K. Abbas. 1998. Functional roles of Fas and Bcl-2-regulated apoptosis of T lymphocytes. *J. Immunol.* 160: 2065–2071.
38. Jaattela, M., and J. Tschopp. 2003. Caspase-independent cell death in T lymphocytes. *Nat. Immunol.* 4: 416–423.
39. Shimizu, S., T. Kanaseki, N. Mizushima, T. Mizuta, S. Arakawa-Kobayashi, C. B. Thompson, and Y. Tsujimoto. 2004. Role of Bcl-2 family proteins in a non-apoptotic programmed cell death dependent on autophagy genes. *Nat. Cell Biol.* 6: 1221–1228.
40. Soriano, M. E., L. Nicolosi, and P. Bernardi. 2004. Desensitization of the permeability transition pore by cyclosporin A prevents activation of the mitochondrial apoptotic pathway and liver damage by tumor necrosis factor- $\alpha$ . *J. Biol. Chem.* 279: 36803–36808.
41. Crabtree, G. R. 2001. Calcium, calcineurin, and the control of transcription. *J. Biol. Chem.* 276: 2313–2316.
42. Perl, A., P. Gergely, Jr., F. Puskas, and K. Banki. 2002. Metabolic switches of T-cell activation and apoptosis. *Antioxid. Redox Signal.* 4: 427–443.
43. Wan, J., D. Martinvalet, X. Ji, C. Lois, S. M. Kaech, U. H. Von Andrian, J. Lieberman, R. Ahmed, and N. Manjunath. 2003. The Bcl-2 family pro-apoptotic molecule, BNIP3 regulates activation-induced cell death of effector cytotoxic T lymphocytes. *Immunology* 110: 10–17.
44. Lamy, L., M. Ticchioni, A. K. Rouquette-Jazdani, M. Samson, M. Deckert, A. H. Greenberg, and A. Bernard. 2003. CD47 and the 19 kDa interacting protein-3 (BNIP3) in T cell apoptosis. *J. Biol. Chem.* 278: 23915–23921.
45. Vande Velde, C., J. Cizeau, D. Dubik, J. Alimonti, T. Brown, S. Israels, R. Hakem, and A. H. Greenberg. 2000. BNIP3 and genetic control of necrosis-like cell death through the mitochondrial permeability transition pore. *Mol. Cell. Biol.* 20: 5454–5468.
46. Grayson, J. M., A. J. Zajac, J. D. Altman, and R. Ahmed. 2000. Increased expression of Bcl-2 in antigen-specific memory CD8<sup>+</sup> T cells. *J. Immunol.* 164: 3950–3954.
47. Pittet, M. J., V. Rubio-Godoy, G. Boley, P. Guillaume, P. Batard, D. Speiser, I. Luescher, J. C. Cerottini, P. Romero, and A. Zippelius. 2003.  $\alpha 3$  domain mutants of peptide/MHC class I multimers allow the selective isolation of high avidity tumor-reactive CD8 T cells. *J. Immunol.* 171: 1844–1849.
48. Schott, E., and H. L. Ploegh. 2002. Mouse MHC class I tetramers that are unable to bind to CD8 reveal the need for CD8 engagement in order to activate naive CD8 T cells. *Eur. J. Immunol.* 32: 3425–3434.
49. Lieberman, S. M., T. Takaki, B. Han, P. Santamaria, D. V. Serreze, and T. P. DiLorenzo. 2004. Individual non-obese diabetic mice exhibit unique patterns of CD8<sup>+</sup> T cell reactivity to three islet antigens, including the newly identified widely expressed dystrophin myotonia kinase. *J. Immunol.* 173: 6727–6734.